MDPI

Data Descriptor

Retinal Fundus Multi-Disease Image Dataset (RFMiD): A Dataset for Multi-Disease Detection Research

Samiksha Pachade [1,*], Prasanna Porwal [1], Dhanshree Thulkar [2], Manesh Kokare [1], Girish Deshmukh [3], Vivek Sahasrabuddhe [4], Luca Giancardo [5], Gwenolé Quellec [6] and Fabrice Mériaudeau [7]

[1] Center of Excellence in Signal and Image Processing, Shri Guru Gobind Singhji Institute of Engineering and Technology, Nanded 431606, India; porwalprasanna@sggs.ac.in (P.P.); mbkokare@sggs.ac.in (M.K.)
[2] Electronics Department, Veermata Jijabai Technological Institute, Mumbai 400019, India; dhanshreethulkar@gmail.com
[3] Eye Clinic, Sushrusha Hospital, Nanded 431601, India; girishnanded@gmail.com
[4] Department of Ophthalmology, Shankarrao Chavan Government Medical College, Nanded 431606, India; smvivek195@gmail.com
[5] Center for Precision Health, School of Biomedical Informatics, University of Texas Health Science Center at Houston (UTHealth), Houston, TX 77030, USA; Luca.Giancardo@uth.tmc.edu
[6] Inserm, UMR 1101, F-29200 Brest, France; gwenole.quellec@inserm.fr
[7] ImViA EA 7535 and ERL VIBOT 6000, Université de Bourgogne, 21078 Dijon, France; fabrice.meriaudeau@u-bourgogne.fr
* Correspondence: 2017pec601@sggs.ac.in

Abstract: The world faces difficulties in terms of eye care, including treatment, quality of prevention, vision rehabilitation services, and scarcity of trained eye care experts. Early detection and diagnosis of ocular pathologies would enable forestall of visual impairment. One challenge that limits the adoption of computer-aided diagnosis tool by ophthalmologists is the number of sight-threatening rare pathologies, such as central retinal artery occlusion or anterior ischemic optic neuropathy, and others are usually ignored. In the past two decades, many publicly available datasets of color fundus images have been collected with a primary focus on diabetic retinopathy, glaucoma, age-related macular degeneration and few other frequent pathologies. To enable development of methods for automatic ocular disease classification of frequent diseases along with the rare pathologies, we have created a new Retinal Fundus Multi-disease Image Dataset (RFMiD). It consists of 3200 fundus images captured using three different fundus cameras with 46 conditions annotated through adjudicated consensus of two senior retinal experts. To the best of our knowledge, our dataset, RFMiD, is the only publicly available dataset that constitutes such a wide variety of diseases that appear in routine clinical settings. This dataset will enable the development of generalizable models for retinal screening.

Dataset: https://riadd.grand-challenge.org/download-all-classes/

Dataset License: CC-BY 4.0

1. Summary

According to the WHO, world report on vision 2019, the total number of visually impaired people worldwide is estimated to be 2.2 billion, from which at least 1 billion cases could have been prevented or are yet to be addressed [1]. Eye screening through visualization of retinal circulation, via color fundus photos, offers a unique opportunity to non-invasively examine systemic microcirculation in the human retina. Detailed clinical observations of characteristic retinal fundus features—not only provide information about

the eye diseases—but also have led to the identification of early indicators of a diverse range of long-term conditions, such as diabetes, stroke, hypertension, arteriosclerosis, cardiovascular, neurodegenerative, and renal and fatty liver diseases [2–4]. Hence, the retina is a potential surrogate organ whose examinations are important not only for the health of the eye but also to determine if there are systemic issues that need attention. Thus, screening of eyes coupled with timely consultation and treatment is a globally trusted policy to avoid vision loss and damage to other parts of the body. Early detection and diagnosis of ocular pathologies in the initial stage of disease progression would enable forestall of visual impairment. Thus, to reduce the socioeconomic burdens of visual loss, development of an automatic disease screening system is important. In the past few decades, larger amount of color fundus images of diabetic patients were collected through Diabetic Retinopathy (DR) screening programs [5–7]. Some datasets were also developed for two other sight-threatening pathologies, Glaucoma [8–10] and Age-related Macular Degeneration (AMD) [11–14]. Patients visiting DR screening programs may also suffer from other diseases, such as Glaucoma and AMD; thus, multi-disease detection is crucial. However, the datasets used for these studies are either private datasets or they include only a few pathologies. But, along with the detection of frequent pathologies, detection and diagnosis of other sight-threatening rare pathologies, like central retinal artery occlusion or anterior ischemic optic neuropathy and others are important. The detection of these rare pathologies is usually ignored that usually occur in routine clinical checkups. This restricts the adoption of automated screening systems by the ophthalmologists. Recent studies highlight importance of efforts in the direction of multi-disease detection [15,16].

To boost the efforts towards development of generalizable retinal screening system, this dataset is available as a part of "Retinal Image Analysis for multi-Disease Detection Challenge (http://biomedicalimaging.org/2021/challenges/)", organized in conjunction with IEEE International Symposium on Biomedical Imaging (ISBI-2021), Nice, France. The data challenge is hosted on Grand Challenges in Biomedical Imaging Platform. Information about data accessibility and specifications is provided in Table 1. This dataset will enable development of techniques/networks for detection/classification of disease(s) in presence of less number of sample cases.

Table 1. Specifications table.

Subject area	Biomedical Imaging, Ophthalmology
More specific subject area	Retinal image analysis for multi-disease detection
Type of data	Image, CSV
How data was acquired	Three different retinal fundus cameras. Model names: TOPCON 3D OCT-2000, Kowa VX-10 and TOPCON TRC-NW300
Data format	Raw and Manual Annotations
Experimental factors	Most of the patients were subjected to mydriasis with one drop of tropicamide at 0.5% concentration
Experimental features	The fundus images were captured with position and orientation of the patient sitting upright with 39 mm (Kowa VX-10) and 40.7 mm (TOPCON 3D OCT-2000 and TOPCON TRC-NW300) distance between lenses and examined eye using non-invasive fundus camera
Data source location	Eye Clinic, Sushrusha Hospital, and Center of Excellence in Signal and Image Processing, SGGS Institute of Engineering and Technology both located in Nanded, (M.S.), India
Data accessibility	https://riadd.grand-challenge.org/download-all-classes/

2. Data Description

The RFMiD is a new publicly available retinal images dataset consisting of 3200 images along with the expert annotations divided into two categories, as follows:

- Screening of retinal images into normal and abnormal (comprising of 45 different types of diseases/pathologies) categories.
- Classification of retinal images into 45 different categories.

The dataset is split into 3 subsets: training 60% (1920 images), evaluation 20% (640 images), and test 20% (640 images) sets. The disease wise stratification on average in training, evaluation and test set is 60 ± 7 %, 20 ± 7%, and 20 ± 5%, respectively. The main motto of this dataset is to provide multiple diseases that appear in routine clinical practice. The labels are provided in three CSV files *RFMiD_Training_Labels.CSV*, *RFMiD_Validation_Labels.CSV*, and *RFMiD_Testing_Labels.CSV*. The information available in the CSV file is illustrated in Figure 1, with each column explanation given as follows:

A. ID: Image identity number.
B. Disease_Risk: Presence of disease/abnormality.
C. DR: Presence of diabetic retinopathy.
D. ARMD: Presence of age-related macular degeneration.
E. MH: Presence of media haze.
F. DN: Presence of drusen.
G. MYA: Presence of myopia.
H. BRVO: Presence of branch retinal vein occlusion.
I. TSLN: Presence of tessellation.
.
.
AU. CL: Presence of collateral.

	A	B	C	D	E	F	G	H	I	J	AU
1	ID	Disease_Risk	DR	ARMD	MH	DN	MYA	BRVO	TSLN	....	CL
2	1	1	1	1	0	0	1	0	0		0
3	2	1	0	0	0	0	0	1	0		0
4	3	1	1	0	1	1	0	0	1		0
5	4	1	0	0	0	0	0	0	0		1
6	5	0	0	0	0	0	0	0	0		0

Figure 1. Sample CSV files.

3. Experimental Design, Materials, and Methods

3.1. Data Acquisition

The retinal images were acquired using three different digital fundus cameras, TOP-CON 3D OCT-2000, Kowa VX-10α, and TOPCON TRC-NW300, all of them centered either on the macula or optic disc. These images are collected from subjects visiting an eye clinic due to a concern for their eye health.

- *Pretreatment of Samples*: Before image acquisition, pupils of most of the subjects were dilated with one drop of tropicamide at 0.5% concentration. The fundus images were captured with position and orientation of the patient sitting upright with 39 mm (Kowa VX–10) and 40.7 mm (TOPCON 3D OCT-2000 and TOPCON TRC-NW300) distance between lenses and examined eye using non-invasive fundus camera.
- *Fundus Camera Specifications*: Regular retinal fundus images were acquired using three different digital fundus cameras. Details of camera model, hardware used, field of view (FOV), resolution, and number of images included in the dataset are given in Table 2.
- *Data Quality*: The dataset is formed by extracting 3200 images from the thousands of examinations done during the period 2009–2020. Both high-quality and low-quality images are selected to make the dataset challenging.

Table 2. Fundus camera specifications.

Model	Hardware	FOV	Resolution (in Pixels)	Number of Images in Dataset
TOPCON 3D OCT-2000	Nikon D7000 digital camera	45°	2144 × 1424	2427
Kowa VX-10α	Nikon D70s digital camera	50°	4288 × 2848	467
TOPCON TRC-NW300	Integrated digital CCD camera	45°	2048 × 1536	306

3.2. Annotation of Images

Initially, all the images were labeled by two ophthalmologists independently. The reference standard for presence of different diseases was assigned based on the comprehensive evaluation of the subjects clinical records and visual fields. If a fundus image shows presence of more than one disease, then multiple labels are assigned to the single image. After the ophthalmologists completed initial labeling of fundus photographs, the leader of the project team checked and confirmed or corrected through consultation from both the ophthalmologists when difference in diagnostic assessments was observed to get adjudicated consensus for the labels.

Table 3 presents number of images per class in the dataset. A brief explanation about the disease/abnormality with their significant visual characteristics of all 45 categories is given below:

Table 3. Stratification according to the diseases.

Sr. No.	Normal/Disease /Marker	# Fundus Images	C1	C2	C3	Sr. No.	Normal/Disease /Marker	# Fundus Images	C1	C2	C3
1	NL	669	333	153	183	24	CRS	54	46	08	00
2	DR	632	519	112	01	25	EDN	24	16	08	00
3	ARMD	169	126	43	00	26	RPEC	32	29	03	00
4	MH	523	425	69	29	27	MHL	17	15	02	00
5	DN	230	198	26	06	28	RP	10	08	02	00
6	MYA	167	137	26	04	29	CWS	08	07	01	00
7	BRVO	119	106	13	00	30	CB	02	01	01	00
8	TSLN	304	247	52	05	31	ODPM	02	02	00	00
9	ERM	26	20	06	00	32	PRH	05	04	01	00
10	LS	79	74	05	00	33	MNF	03	03	00	00
11	MS	27	25	02	00	34	HR	01	01	00	00
12	CSR	61	58	03	00	35	CRAO	04	04	00	00
13	ODC	445	357	52	36	36	TD	09	07	00	02
14	CRVO	45	43	02	00	37	CME	07	07	00	00
15	TV	10	09	01	00	38	PTCR	06	06	00	00
16	AH	25	19	04	02	39	CF	06	04	02	02
17	ODP	115	94	20	01	40	VH	04	04	00	00
18	ODE	96	91	05	00	41	MCA	01	01	00	00
19	ST	11	07	03	01	42	VS	04	04	00	00
20	AION	26	25	01	00	43	BRAO	04	03	01	00
21	PT	17	15	02	00	44	PLQ	02	01	01	00
22	RT	25	23	02	00	45	HPED	01	01	00	00
23	RS	71	71	00	00	46	CL	02	01	01	00

C1: TOPCON 3D OCT-2000: C2: Kowa VX-10α; C3: TOPCON TRC-NW300.

Diabetic retinopathy (DR) is a microvascular complication of diabetes mellitus and is a leading cause of vision loss in the elderly and working population. The image is labeled as DR if it shows any of the following clinical findings: microaneurysms, retinal dot and blot hemorrhage, hard exudates or cotton wool spots (see Figure 2a) [17].

Age-related macular degeneration (ARMD) is a progressive chronic disease of the central retina that usually develops in old age people and is a leading cause of vision loss. The image is labeled as ARMD if it shows any of the following clinical findings: multiple drusen in macular region, geographic atrophy (see Figure 2b) involving the fovea, features of neovascular age-related macular degeneration [18].

Media Haze (MH): The opacity of media can be a hallmark for the presence of cataracts, vitreous opacities, corneal edema or small pupils [19]. Moreover, some other artifacts may be introduced as a result of acquisition procedures, such as eyelash artifacts and artifacts introduced by the instrument. All these are labeled under the category MH, as shown in Figure 2c.
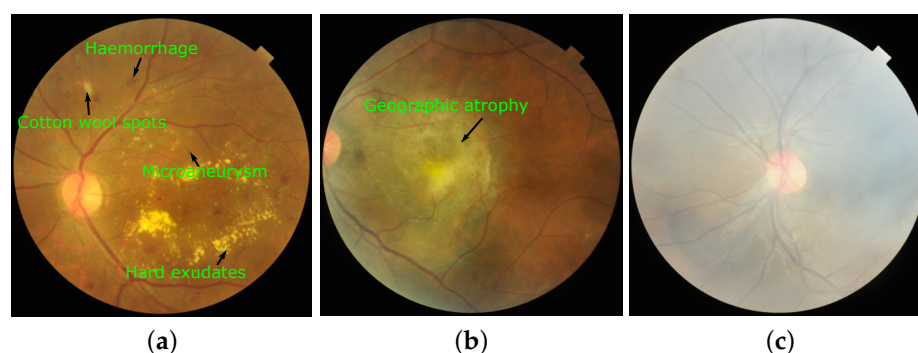

Figure 2. Images of (**a**) diabetic retinopathy (DR), (**b**) age-related macular degeneration (ARMD), and (**c**) media haze (MH) based on their visual characteristics.

Drusens (DN) are yellow or white extracellular deposits (shown in Figure 3a) located between the retinal pigment epithelium (RPE) and Bruch's membrane. They naturally occur in the aged population. The presence of drusen is a hallmark and early sign of significant risk of age-related macular degeneration, geographic atrophy, choroidal neovascularization, and development of RPE abnormalities [20].

Myopia (MYA) is characterized by degenerative changes in the choroid, sclera, and RPE (see Figure 3b) [21]. Vision loss due to myopia can be progressive and irreversible.

Branch retinal vein occlusion (BRVO) is the most common visual disorder causing visual blurring in the peripheral region. The visual signs in the retina can be any of the following: occlusion of one or more branches of the central retinal vein, dot and blot hemorrhage, flame-shaped hemorrhage, soft and hard exudates, retinal edema, and dilated, tortuous vein [22]. These visual signs are shown in Figure 3c.
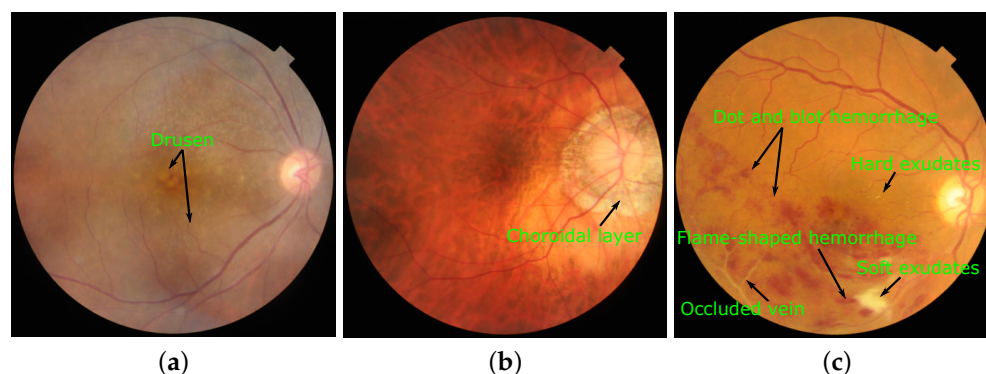

Figure 3. Images of (**a**) drusens (DN), (**b**) myopia (MYA), and (**c**) branch retinal vein occlusion (BRVO) based on their visual characteristics.

Tessellation (TSLN) in the fundus images appears due to the thinning of the RPE and choriocapillaris. The choroidal vessels (shown in Figure 4a) are visible due to the reduced

density of the pigments. Mild tessellation occurs with aging and it might be present in normal retinal image. Moderate tessellations are related to myopia [23]. In the database, the label tessellation is given to images with moderate tessellations.

Epiretinal membrane (ERM) is a thin sheet of glial cells that appears as an irregular light reflex on the surface of macular region of the retina as shown in Figure 4b. Symptoms associated with ERM are loss of central vision and decreased visual acuity [24].

Laser scars (LS) indicate that patient had underwent laser therapy which is predominately preferred treatment method to stop the progression of vascular leaks [25]. This treatment results in circular or irregular shaped scars on the retinal surface as shown in Figure 4c.
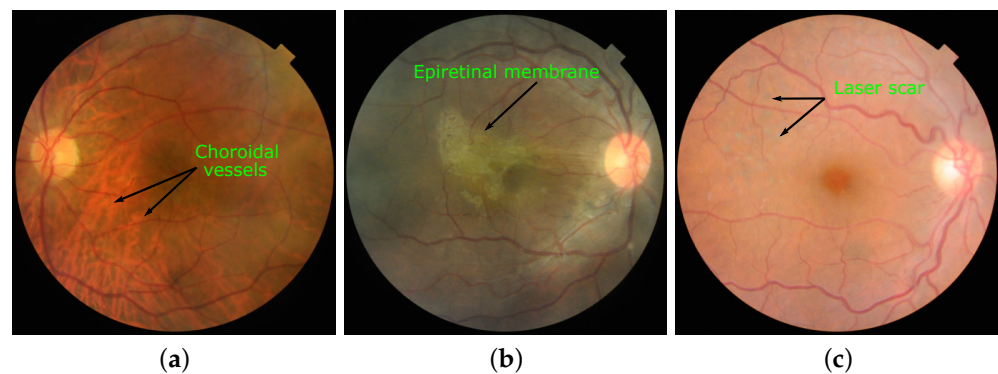

(**a**) (**b**) (**c**)

Figure 4. Images of (**a**) tessellation (TSLN), (**b**) epiretinal membrane (ERM), and (**c**) laser scars (LS) based on their visual characteristics.

Macular scar (MS) is either caused by infection or inflammatory intraocular reaction that causes slight injury to RPE shown in Figure 5a. It is responsible for complications or decreased vision [26].

Central serous retinopathy (CSR) is characterized as a round serous detachment of the neurosensory retina from the underlying RPE. The subretinal fluid (see Figure 5b) is a clinical indicator for the presence of CSR. The vision loss depends on the amount of detachment of neurosensory retina [27].

Optic disc cupping (ODC) is the thinning of neuroretinal rim such that optic disc appears excavated as shown in Figure 5c. Pathological ODC is generally referred to as glaucoma. However, several other non-glaucomatous diseases, such as arteritic anterior ischemic optic neuropathy and central retinal vein occlusion, also result in ODC [28]. Thus, it is very important to separately evaluate ODC.
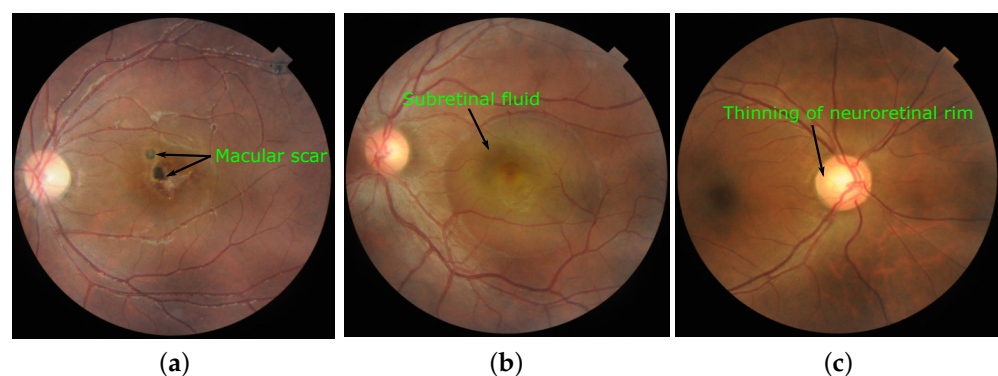

(**a**) (**b**) (**c**)

Figure 5. Images of (**a**) macular scar (MS), (**b**) Central serous retinopathy (CSR), and (**c**) optic disc cupping (ODC) based on their visual characteristics.

Central retinal vein occlusion (CRVO) is the occlusion of central retinal vein with a start point at or proximal to the lamina cribrosa of the optic nerve. The clinical signs are presence of flame-shaped hemorrhages, as shown in Figure 6a. It may develop permanent, severe, visual impairment [29].

Tortuous vessels (TV) is characterized by pattern of marked tortuosity (that appears dilated and follow a serpentine path see Figure 6b) of the retinal blood vessels. It is associated with diseases, like hypertension, diabetes, and other genetic disorders [30].

Asteroid hyalosis (AH) is a condition in which numerous astroid bodies (white small spherical particles see Figure 6c) are dispersed in vitreous. The presence of AH may be associated with diabetes, hyperlipidemia, or hypertension [31].
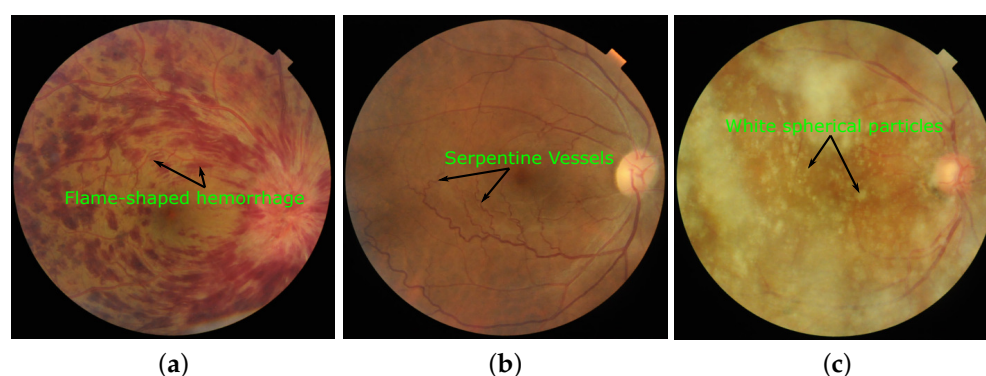

(**a**)　　　　　　　　　　　(**b**)　　　　　　　　　　　(**c**)

Figure 6. Images of (**a**) central retinal vein occlusion (CRVO), (**b**) tortuous vessels (TV), and (**c**) asteroid hyalosis (AH) based on their visual characteristics.

Optic disc pallor (ODP) refers to pale yellow discoloration of the optic disc, as well as absence of many small vessels, as shown in Figure 7a. Vision loss due to ODP depends on the degree of pallor [32].

Optic disc edema (ODE) includes findings, such as papilledema, papillitis, and choked or swollen discs (see Figure 7b). It is a classic marker that represent initial signs of anterior ischemic optic neuropathy [33], this may eventually lead to loss of vision.

Optociliary **shunt (ST)** vessels are vessels on the optic nerve head that connect the retinal venous system to the choroid. The clinical findings are presence of prepapillary vascular loops (see Figure 7c) or optociliary shunt vessels. It causes slowly progressive vision loss [34].
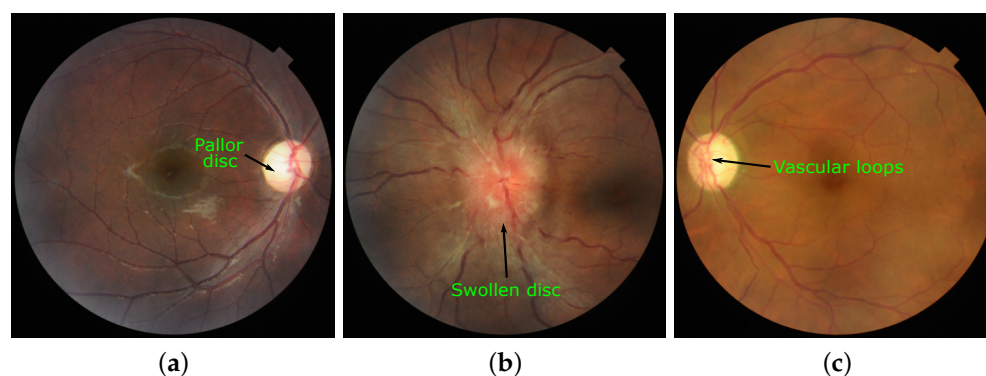

(**a**)　　　　　　　　　　　(**b**)　　　　　　　　　　　(**c**)

Figure 7. Images of (**a**) optic disc pallor (ODP), (**b**) optic disc edema (ODE), and (**c**) optociliary shunt (ST) based on their visual characteristics.

Anterior ischemic optic neuropathy (AION) is caused by the damage of anterior (front) part of optic nerve resulting in ischemia (decrease in the blood supply) as illustrated

in Figure 8a. In middle-aged and elderly people, it is one of the leading cause of seriously impaired vision or blindness [35].

Parafoveal telangiectasia (PT) is a clinical condition characterized by yellow, lipid-rich exudation or parafoveal graying or abnormalities from distention and tortuous blood vessels (ectatic) and incompetent retinal capillaries in the juxtafoveolar region (see Figure 8b). It is responsible for central vision loss [36,37].

Retinal traction (RT) detachment is separation of the neurosensory retina from the RPE due to traction (see Figure 8c). Under the label RT, images showing presence of traction and retinal traction detachment are included [38].
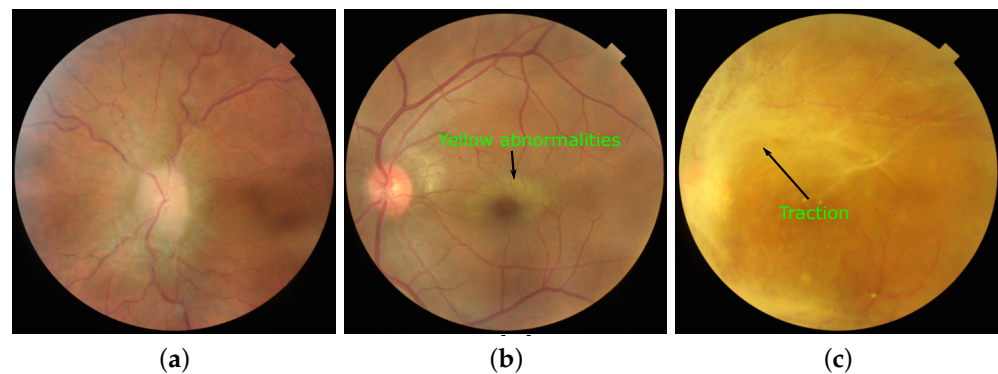

Figure 8. Images of (**a**) anterior ischemic optic neuropathy (AION), (**b**) parafoveal telangiectasia (PT), and (**c**) retinal traction (RT) based on their visual characteristics.

Retinitis (RS) is characterized by the presence of any of the following clinical signs: vitreous inflammation, macular star, intraretinal hemorrhage, phlebitis, arteritis, and hyperemic disc, as shown in Figure 9a. The most common visual loss in this case is central vision loss [39].

Chorioretinitis (CRS) causes inflammation of choroid and retina which results in vision-threatening complications. It is usually caused by infections, like toxoplasmosis and cytomegalovirus, as shown in Figure 9b [40].
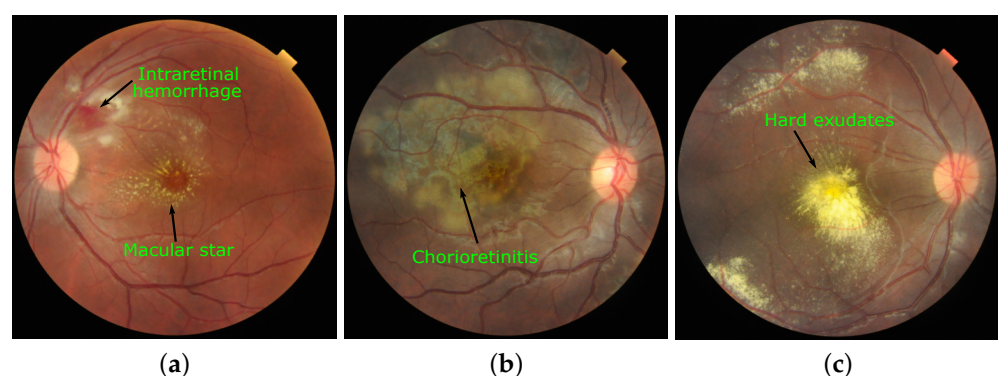

Figure 9. Images of (**a**) retinitis (RS), (**b**) chorioretinitis (CRS), and (**c**) exudation (EDN) based on their visual characteristics.

Exudation (EDN): The hard exudates are white or yellowish lipid deposits with sharp edges as shown in Figure 9c. Circinate retinopathy is a clinical condition marked by a circle of exudates surrounding the macular area [41]. Exudative maculopathy is a clinical condition marked by masses exudates in the macular region [42]. Macular star is a star-like formation of exudates in the macular region [43]. All these conditions are labeled under category EDN.

Retinal pigment epithelium changes (RPEC) are characterized by the structural changes, such as increased thickness of Bruch's membrane, loss of melanin granules, accumulation of lipofuscin, formation of drusen, increase in the density of residual bodies, accumulation of basal deposits on or within Bruch's membrane, and disorganization of the basal infoldings and microvilli atrophy (see Figure 10a). These changes lead to severe visual loss [44].

Macular hole (MHL) is a small retinal break located in the center of the fovea (see Figure 10b), causing significant vision impairment [45].

In **retinitis pigmentosa (RP)**, retina progressively degenerates. The visual signs are bone-spicule deposits and arterial narrowing as shown in Figure 10c. It causes night blindness, which eventually leads to complete blindness [46].
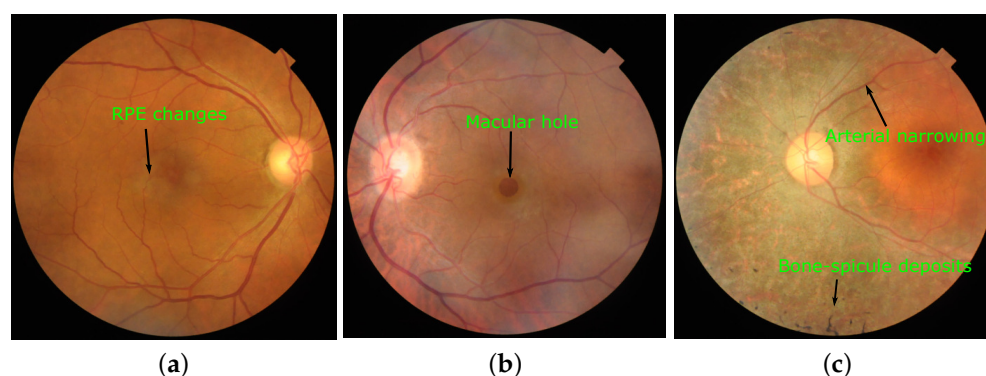

(**a**) (**b**) (**c**)

Figure 10. Images of (**a**) retinal pigment epithelium changes (RPEC), (**b**) macular hole (MHL), and (**c**) retinitis pigmentosa (RP) based on their visual characteristics.

Cotton-wool spots (CWS) are whitish, fluffy patches appearing on the surface of retina as shown in Figure 11a. They are manifestations of common retinal diseases, like diabetes mellitus, acquired immunodeficiency syndrome, and systemic hypertension [47].
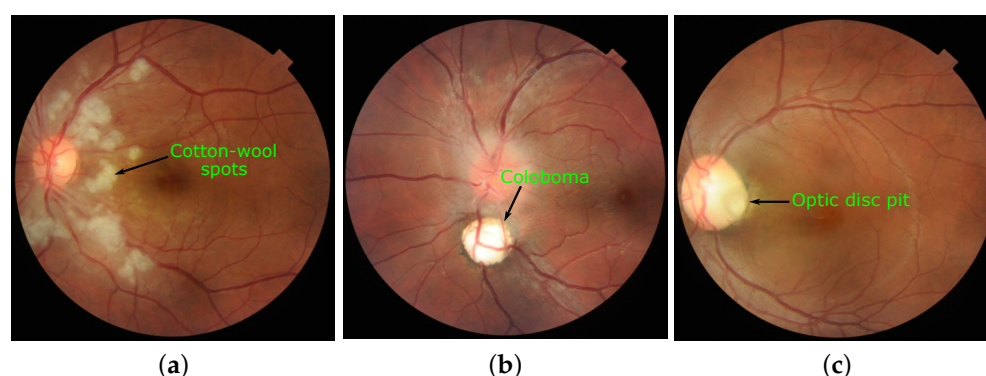

(**a**) (**b**) (**c**)

Figure 11. Images of (**a**) cotton-wool spots (CWS), (**b**) coloboma (CB), and (**c**) optic disc pit maculopathy (ODPM) based on their visual characteristics.

Coloboma (CB) is marked as a missing portion of tissue in both the choroid and retina at the time of birth. It can be visualized as a white zone (see Figure 11b) of the retinal fundus images. It is responsible for the loss of visual fields, cataract and retinal detachment may occur [48].

Optic disc pit maculopathy (ODPM): Optic disc pit is a rare unilateral and sporadic congenital abnormality of the optic disc as shown in Figure 11c. ODPM is characterized by intraretinal and subretinal fluid at the macula, causing progressive visual loss [49].

Preretinal hemorrhage (PRH) usually appears as a boat-shaped hemorrhage (see Figure 12a) which obscures the underlying retina. Underlying causes include bleeding from

neovascularization, vascular occlusion, hypertensive retinopathy, retinal tear, posterior vitreous detachment and rupture of the internal limiting membrane [50].

Myelinated nerve fibers (MNF) are inborn irregularities that are characterized as gray-white opaque lesions with feathery edges as shown in Figure 12b. They may be located along nerve fibers of the optic disc or elsewhere on the retina. It is associated with diseases, like pituitary tumor, embolism of the central retinal, multiple sclerosis, and optic nerve atrophy [51].

Hemorrhagic retinopathy (HR) is a particular form of retinopathy which is hemorrhagic in nature as shown in Figure 12c. It is associated with the diabetes, hypertension, and occlusion of the central vein [52].
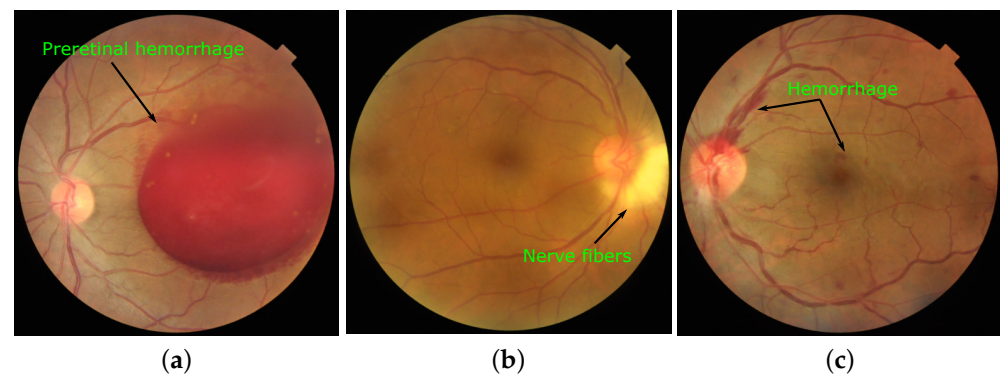

(a) (b) (c)

Figure 12. Images of (**a**) preretinal hemorrhage (PRH), (**b**) myelinated nerve fibers (MNF), and (**c**) hemorrhagic retinopathy (HR) based on their visual characteristics.

Central retinal artery occlusion (CRAO) occurs due to embolus blocking the central retinal artery. It is characterized by pale, whitening, and retinal swelling as shown in Figure 13a. It is responsible for sudden, catastrophic visual loss [53].

Tilted disc (TD) is tilting of the optic disc and usually occurs bilaterally, as shown in Figure 13b. It is associated with high myopia [54].

Cystoid macular edema (CME) is characterized by the multiple cyst-like (cystoid) areas in the macula and causes retinal edema (swelling), as shown in Figure 13c. It causes decreased or blurred central vision [55].
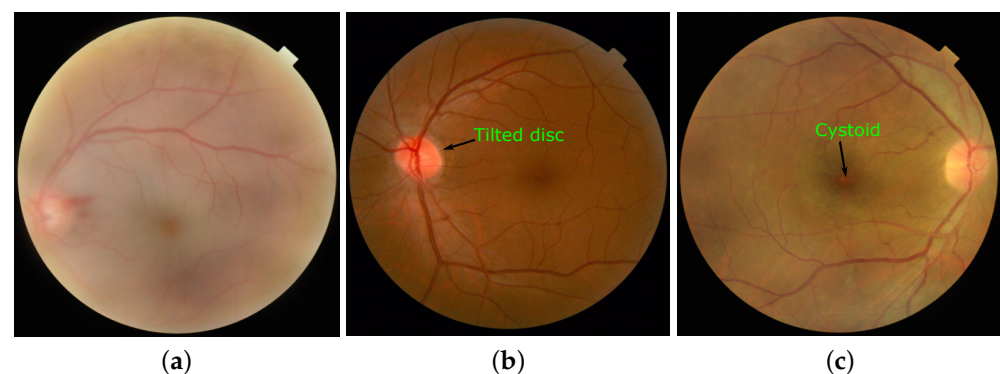

(a) (b) (c)

Figure 13. Images of (**a**) central retinal artery occlusion (CRAO), (**b**) tilted disc (TD), and (**c**) cystoid macular edema (CME) based on their visual characteristics.

Post-traumatic choroidal rupture (PTCR) are breaks in the choroid, Bruch's membrane, and RPE which occurs as an effect of blunt ocular trauma as shown in Figure 14a. It leads to serous macular or haemorrhagic detachment [56].

Choroidal folds (CF) is a series of dark and light lines (see Figure 14b) usually temporal and confined to the posterior pole. They occur after some surgical procedures and in a variety of ocular diseases [57].

Vitreous hemorrhage (VH) is extravasated blood in one of the spaces created around the vitreous body. It is a result of neovascularization or retinal tears or blood vessel bleeding, as shown in Figure 14c [58].
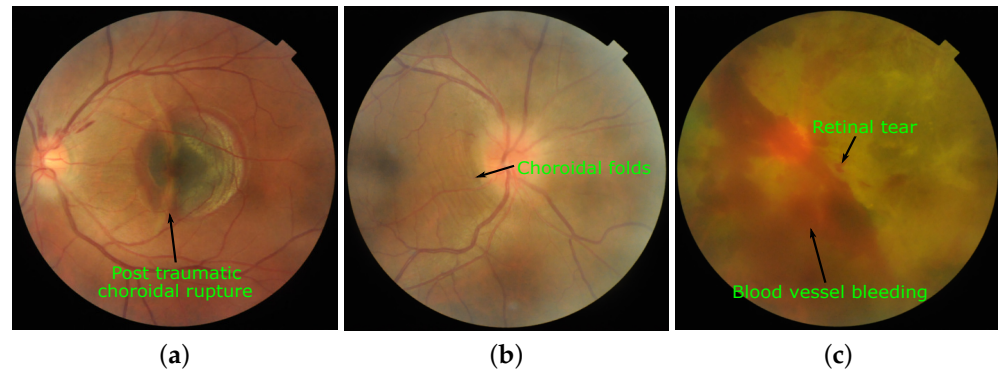

(**a**)   (**b**)   (**c**)

Figure 14. Images of (**a**) post-traumatic choroidal rupture (PTCR), (**b**) choroidal folds (CF), and (**c**) vitreous hemorrhage (VH) based on their visual characteristics.

Macroaneurysm (MCA) is fusiform or round dilation of the retinal arterioles which occur in the temporal retina. It is generally unilateral and surrounded by circinate exudation. The central vision loss is due to the presence of edema, hemorrhage, and exudation, as shown in Figure 15a [59].

Vasculitis (VS) is inflammation of retinal blood vessels. It is characterized by white sheathing due to the presence of exudates around retinal blood vessels or cuffing of the affected vessels as shown in Figure 15b. It causes exudation, retinal swelling, and macular edema [60].

Branch retinal artery occlusion (BRAO) occurs due to acute retinal artery obstructions (see Figure 15c). It may cause sectoral visual field loss [61].
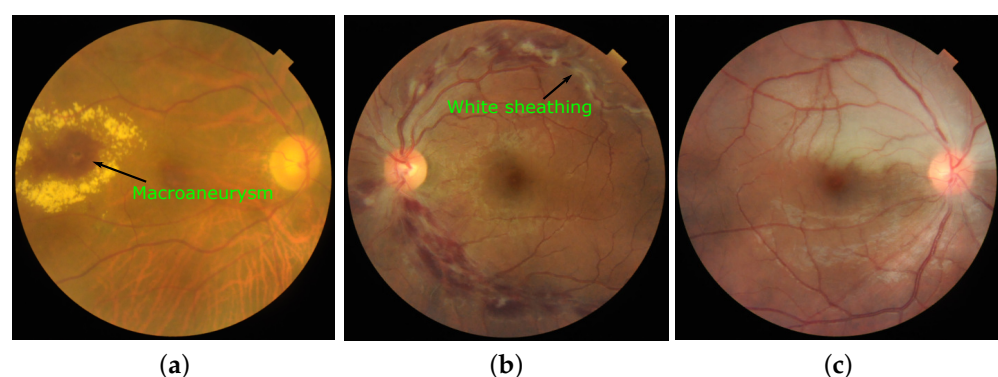

(**a**)   (**b**)   (**c**)

Figure 15. Images of (**a**) macroaneurysm (MCA), (**b**) vasculitis (VS), and (**c**) branch retinal artery occlusion (BRAO) based on their visual characteristics.

Plaque (PLQ) is bright orange-yellow in color and are located in retinal arteries as shown in Figure 16a. If the plaque is present in retina then refer the patient for investigation of the cardiovascular system [62].

In **hemorrhagic pigment epithelial detachment (HPED)** the pigment epithelium is separated due to hemorrhage (see Figure 16b) from the Bruch's membrane. It is a predictive feature for the presence of polypoidal choroidal vasculopathy or choroidal neovascularization [63].

Collateral (CL) is new retinal vessels (see Figure 16c) developed within the framework of existing vessel network. It is a hallmark for the disease, like optic disc drusen, high myopia, and diabetes [64].
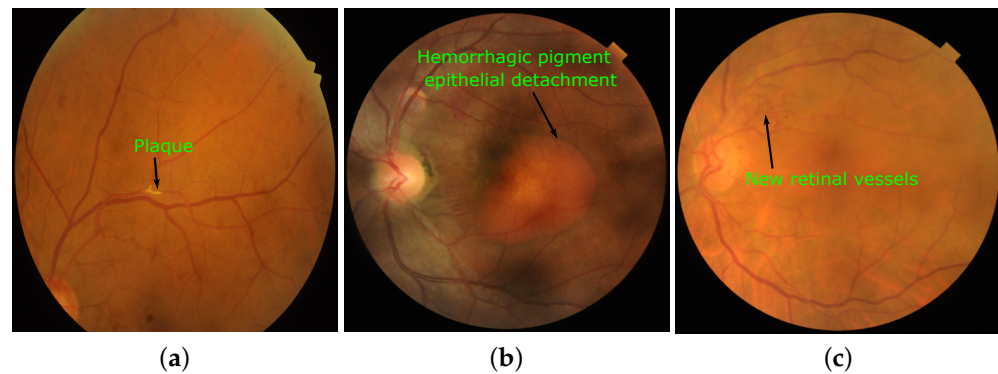

(**a**) (**b**) (**c**)

Figure 16. Images of (**a**) plaque (PLQ), (**b**) hemorrhagic pigment epithelial detachment (HPED), and (**c**) collateral (CL) based on their visual characteristics.

This dataset represents a number of images with respect to rare pathologies, and recent techniques ([15,16]) have shown the ways to address this challenge, and more research work can be done in this direction to get results on this and other similar datasets.

Author Contributions: Conceptualization, S.P., P.P., and M.K.; Methodology, S.P., G.D., and V.S.; Resources, G.D.; Data Curation, S.P. and D.T.; Disease Grading, G.D. and V.S.; Annotation Validation, G.D. and V.S.; Investigation, M.K. and F.M.; Writing—Original Draft Preparation, S.P.; Writing—Review & Editing, P.P, M.K., G.D., V.S., L.G., G.Q., and F.M.; Visualization, S.P. and P.P.; Supervision, M.K. and F.M.; Project Administration, M.K. and F.M. All authors have read and agreed to the published version of the manuscript.

Institutional Review Board Statement: The study was conducted according to the ethics of clinical practices and medical research, and approved by the Institutional Review Board of Shri Guru Gobind Singhji Institute of Engineering and Technology, Nanded, India.

Informed Consent Statement: Informed consent was obtained from all subjects involved in the study.

Data Availability Statement: This dataset is available for download at: https://riadd.grand-challenge.org/download-all-classes/.

Conflicts of Interest: The authors declare no conflict of interest.

References

1. Who Launches First World Report on Vision. Available online: https://www.who.int/blindness/Vision2020_report.pdf (accessed on 29 January 2021).
2. MacGillivray, T.; Trucco, E.; Cameron, J.; Dhillon, B.; Houston, J.; Van Beek, E. Retinal imaging as a source of biomarkers for diagnosis, characterization and prognosis of chronic illness or long-term conditions. *Br. J. Radiol.* **2014**, *87*, 20130832. [CrossRef] [PubMed]
3. Yang, W.; Xu, H.; Yu, X.; Wang, Y. Association between retinal artery lesions and nonalcoholic fatty liver disease. *Hepatol. Int.* **2015**, *9*, 278–282. [CrossRef] [PubMed]
4. Chang, Y.S.; Weng, S.F.; Chang, C.; Wang, J.J.; Tseng, S.H.; Wang, J.Y.; Jan, R.L. Risk of retinal vein occlusion following end-stage renal disease. *Medicine* **2016**, *95*, e3474. [CrossRef] [PubMed]
5. Porwal, P.; Pachade, S.; Kamble, R.; Kokare, M.; Deshmukh, G.; Sahasrabuddhe, V.; Meriaudeau, F. Indian diabetic retinopathy image dataset (IDRiD): A database for diabetic retinopathy screening research. *Data* **2018**, *3*, 25. [CrossRef]

6.   Decencière, E.; Zhang, X.; Cazuguel, G.; Lay, B.; Cochener, B.; Trone, C.; Gain, P.; Ordonez, R.; Massin, P.; Erginay, A.; et al. Feedback on a publicly distributed image database: The Messidor database. *Image Anal. Stereol.* **2014**, *33*, 231–234. [CrossRef]

7.   Cuadros, J.; Bresnick, G. EyePACS: An adaptable telemedicine system for diabetic retinopathy screening. *J. Diabetes Sci. Technol.* **2009**, *3*, 509–516. [CrossRef]

8.   Sivaswamy, J.; Krishnadas, S.; Chakravarty, A.; Joshi, G.; Tabish, A.S. A comprehensive retinal image dataset for the assessment of glaucoma from the optic nerve head analysis. *JSM Biomed. Imaging Data Pap.* **2015**, *2*, 1004.

9.   Fumero, F.; Alayón, S.; Sanchez, J.L.; Sigut, J.; Gonzalez-Hernandez, M. RIM-ONE: An open retinal image database for optic nerve evaluation. In Proceedings of the 2011 24th International Symposium on Computer-Based Medical Systems (CBMS), Bristol, UK, 27–30 June 2011; pp. 1–6.

10.   Orlando, J.I.; Fu, H.; Breda, J.B.; van Keer, K.; Bathula, D.R.; Diaz-Pinto, A.; Fang, R.; Heng, P.A.; Kim, J.; Lee, J.; et al. Refuge challenge: A unified framework for evaluating automated methods for glaucoma assessment from fundus photographs. *Med. Image Anal.* **2020**, *59*, 101570. [CrossRef]

11.   Farnell, D.J.; Hatfield, F.; Knox, P.; Reakes, M.; Spencer, S.; Parry, D.; Harding, S.P. Enhancement of blood vessels in digital fundus photographs via the application of multiscale line operators. *J. Frankl. Inst.* **2008**, *345*, 748–765. [CrossRef]

12.   Hoover, A. STARE Database. 1975. Available online: https://cecas.clemson.edu/~ahoover/stare/ (accessed on 29 January 2021).

13.   Cohen, S. Retina Gallery Full Sized Retina Images. 2017. Available online: https://www.retinagallery.com/ (accessed on 29 January 2021).

14.   Age-Related Eye Disease Study Research Group. A randomized, placebo-controlled, clinical trial of high-dose supplementation with vitamins C and E, beta carotene, and zinc for age-related macular degeneration and vision loss: AREDS report no. 8. *Arch. Ophthalmol.* **2001**, *119*, 1417. [CrossRef]

15.   Choi, J.Y.; Yoo, T.K.; Seo, J.G.; Kwak, J.; Um, T.T.; Rim, T.H. Multi-categorical deep learning neural network to classify retinal images: A pilot study employing small database. *PLoS ONE* **2017**, *12*, e0187336. [CrossRef] [PubMed]

16.   Quellec, G.; Lamard, M.; Conze, P.H.; Massin, P.; Cochener, B. Automatic detection of rare pathologies in fundus photographs using few-shot learning. *Med. Image Anal.* **2020**, *61*, 101660. [CrossRef] [PubMed]

17.   Wong, T.Y.; Cheung, C.M.G.; Larsen, M.; Sharma, S.; Simó, R. Diabetic retinopathy. *Nat. Rev. Dis. Prim.* **2016**, *2*, 16012. [CrossRef] [PubMed]

18.   Lim, L.S.; Mitchell, P.; Seddon, J.M.; Holz, F.G.; Wong, T.Y. Age-related macular degeneration. *Lancet* **2012**, *379*, 1728–1738. [CrossRef]

19.   Chen, W.S.; Friberg, T.R.; Eller, A.W.; Medina, C. Advances in retinal imaging of eyes with hazy media: Further Studies. *Investig. Ophthalmol. Vis. Sci.* **2011**, *52*, 4036–4036.

20.   Johnson, P.T.; Lewis, G.P.; Talaga, K.C.; Brown, M.N.; Kappel, P.J.; Fisher, S.K.; Anderson, D.H.; Johnson, L.V. Drusen-associated degeneration in the retina. *Investig. Ophthalmol. Vis. Sci.* **2003**, *44*, 4481–4488. [CrossRef] [PubMed]

21.   Morgan, I.G.; Ohno-Matsui, K.; Saw, S.M. Myopia. *Lancet* **2012**, *379*, 1739–1748. [CrossRef]

22.   Rehak, J.; Rehak, M. Branch retinal vein occlusion: pathogenesis, visual prognosis, and treatment modalities. *Curr. Eye Res.* **2008**, *33*, 111–131. [CrossRef]

23.   Ohno-Matsui, K.; Kawasaki, R.; Jonas, J.B.; Cheung, C.M.G.; Saw, S.M.; Verhoeven, V.J.; Klaver, C.C.; Moriyama, M.; Shinohara, K.; Kawasaki, Y.; et al. International photographic classification and grading system for myopic maculopathy. *Am. J. Ophthalmol.* **2015**, *159*, 877–883. [CrossRef]

24.   Foos, R.Y. Vitreoretinal juncture—Simple epiretinal membranes. *Albrecht Von Graefes Arch. Für Klin. Und Exp. Ophthalmol.* **1974**, *189*, 231–250. [CrossRef]

25.   Zhang, W.; Liu, H.; Rojas, M.; Caldwell, R.W.; Caldwell, R.B. Anti-inflammatory therapy for diabetic retinopathy. *Immunotherapy* **2011**, *3*, 609–628. [CrossRef] [PubMed]

26.   Bahia-Oliveira, L.M.; Rangel, A.L.; Boechat, M.S.; Mangiavacchi, B.M.; Martins, L.M.; Ferraz, F.B.; Almeida, M.B.; Peixoto, E.M.W.; Vieira, F.P.; Peixe, R.G. Immunological and immunogenetic parameters on the diversity of ocular toxoplasmosis: evidence to support morphological criteria to classify retinal/retinochoroidal scar lesions in epidemiologic surveys. In *Toxoplasmosis-Recent Advances*; IntechOpen: London, UK 2012.

27.   Chuang, E.; Sharp, D.; Fitzke, F.; Kemp, C.; Holden, A.; Bird, A. Retinal dysfunction in central serous retinopathy. *Eye* **1987**, *1*, 120–125. [CrossRef] [PubMed]

28.   Zhang, Y.X.; Huang, H.B.; Wei, S.H. Clinical characteristics of nonglaucomatous optic disc cupping. *Exp. Ther. Med.* **2014**, *7*, 995–999. [CrossRef] [PubMed]

29.   Quinlan, P.M.; Elman, M.J.; Bhatt, A.K.; Mardesich, P.; Enger, C. The natural course of central retinal vein occlusion. *Am. J. Ophthalmol.* **1990**, *110*, 118–123. [CrossRef]

30.   Sutter, F.K.; Helbig, H. Familial retinal arteriolar tortuosity: A review. *Surv. Ophthalmol.* **2003**, *48*, 245–255. [CrossRef]

31.   Wang, M.; Kador, P.F.; Wyman, M. Structure of asteroid bodies in the vitreous of galactose-fed dogs. *Mol. Vis.* **2006**, *12*, 283–289.

32.   Schwartz, B. Cupping and pallor of the optic disc. *Arch. Ophthalmol.* **1973**, *89*, 272–277. [CrossRef]

33.   Van Stavern, G.P. Optic disc edema. In *Seminars in Neurology*; Thieme Medical Publishers, Inc.: New York, NY, USA; Seventh Avenue: New York, NY, USA, 2007; Volume 27, pp. 233–243.

34.   Haskes, C.; Haskes, L.P. Acquired optociliary shunt vessels and their clinical occurrences. *Clin. Eye Vis. Care* **1995**, *7*, 69–77. [CrossRef]

35. Hayreh, S.S. Management of ischemic optic neuropathies. *Indian J. Ophthalmol.* **2011**, *59*, 123. [CrossRef]

36. Nowilaty, S.R.; Al-Shamsi, H.N.; Al-Khars, W. Idiopathic juxtafoveolar retinal telangiectasis: A current review. *Middle East Afr. J. Ophthalmol.* **2010**, *17*, 224. [CrossRef]

37. Pathengay, A.; Jindal, A.; Choudhury, H. A New Clinical Sign in Parafoveal Telangiectasia. *Investig. Ophthalmol. Vis. Sci.* **2014**, *55*, 5949–5949.

38. Mishra, C.; Tripathy, K. Retinal Traction Detachment. Statpearls [Internet]. 2020. Available online: https://www.ncbi.nlm.nih.gov/books/NBK558952/ (accessed on 29 January 2021).

39. Sivakumar, R.R.; Prajna, L.; Arya, L.K.; Muraly, P.; Shukla, J.; Saxena, D.; Parida, M. Molecular diagnosis and ocular imaging of West Nile virus retinitis and neuroretinitis. *Ophthalmology* **2013**, *120*, 1820–1826. [CrossRef] [PubMed]

40. Geetha, R.; Tripathy, K. Chorioretinitis. StatPearls [Internet]. 2019. Available online: https://www.ncbi.nlm.nih.gov/books/NBK430685/ (accessed on 29 January 2021).

41. Spalter, H.F. Photocoagulation of circinate maculopathy in diabetic retinopathy. *Am. J. Ophthalmol.* **1971**, *71*, 242–250. [CrossRef]

42. Chowdhury, T.; Hopkins, D.; Dodson, P.; Vafidis, G. The role of serum lipids in exudative diabetic maculopathy: Is there a place for lipid lowering therapy? *Eye* **2002**, *16*, 689–693. [CrossRef] [PubMed]

43. Brazis, P.W.; Lee, A.G. Optic disk edema with a macular star. In *Mayo Clinic Proceedings*; Elsevier: Amsterdam, The Netherlands, 1996; Volume 71, pp. 1162–1166.

44. Bonilha, V.L. Age and disease-related structural changes in the retinal pigment epithelium. *Clin. Ophthalmol.* **2008**, *2*, 413. [CrossRef] [PubMed]

45. Bikbova, G.; Oshitari, T.; Baba, T.; Yamamoto, S.; Mori, K. Pathogenesis and management of macular hole: Review of current advances. *J. Ophthalmol.* **2019**, *2019*, 3467381. [CrossRef]

46. Ferrari, S.; Di Iorio, E.; Barbaro, V.; Ponzin, D.; Sorrentino, S.F.; Parmeggiani, F. Retinitis pigmentosa: Genes and disease mechanisms. *Curr. Genom.* **2011**, *12*, 238–249.

47. Ioannides, A.; Georgakarakos, N.D.; Elaroud, I.; Andreou, P. Isolated cotton-wool spots of unknown etiology: Management and sequential spectral domain optical coherence tomography documentation. *Clin. Ophthalmol.* **2011**, *5*, 1431. [CrossRef]

48. Wang, K.; Hilton, G. Retinal detachment associated with coloboma of the choroid. *Trans. Am. Ophthalmol. Soc.* **1985**, *83*, 49.

49. Georgalas, I.; Ladas, I.; Georgopoulos, G.; Petrou, P. Optic disc pit: A review. *Graefe's Arch. Clin. Exp. Ophthalmol.* **2011**, *249*, 1113–1122. [CrossRef]

50. Kuruvilla, O.; Munie, M.; Shah, M.; Desai, U.; Miller, J.A.; Ober, M.D. Nd: YAG membranotomy for preretinal hemorrhage secondary to valsalva retinopathy. *Saudi J. Ophthalmol.* **2014**, *28*, 145–151. [CrossRef] [PubMed]

51. Straatsma, B.R.; Foos, R.Y.; Heckenlively, J.R.; Taylor, G.N. Myelinated retinal nerve fibers. *Am. J. Ophthalmol.* **1981**, *91*, 25–38. [CrossRef]

52. Moss, H.B.; Jara, V.A.K.; Slakter, J.S.; Brucker, A.J.; Rabb, M.F.; Landers, M.B. Clinical Features Of Unilateral Hemorrhagic Retinopathy: A New Retinal Entity? *Investig. Ophthalmol. Vis. Sci.* **2012**, *53*, 5199–5199.

53. Hayreh, S.S.; Zimmerman, M.B. Central retinal artery occlusion: visual outcome. *Am. J. Ophthalmol.* **2005**, *140*, 376. [CrossRef] [PubMed]

54. Dorrell, D. The tilted disc. *Br. J. Ophthalmol.* **1978**, *62*, 16–20. [CrossRef] [PubMed]

55. Irvine, A.R. Cystoid maculopathy. *Surv. Ophthalmol.* **1976**, *21*, 1–17. [CrossRef]

56. Chanana, B.; Azad, R.; Kumar, N. Intravitreal bevacizumab for subfoveal choroidal neovascularization secondary to traumatic choroidal rupture. *Eye* **2009**, *23*, 2125–2126. [CrossRef] [PubMed]

57. Cangemi, F.E.; Trempe, C.L.; Walsh, J.B. Choroidal folds. *Am. J. Ophthalmol.* **1978**, *86*, 380–387. [CrossRef]

58. Lascu, R. Vitreous Hemorrhage. *Acta Med. Transilv.* **2014**, *19*, 3–39.

59. Yamanaka, E.; Ohguro, N.; Kubota, A.; Yamamoto, S.; Nakagawa, Y.; Tano, Y. Features of retinal arterial macroaneurysms in patients with uveitis. *Br. J. Ophthalmol.* **2004**, *88*, 884–886. [CrossRef]

60. El-Asrar, A.M.A.; Herbort, C.P.; Tabbara, K.F. Differential diagnosis of retinal vasculitis. *Middle East Afr. J. Ophthalmol.* **2009**, *16*, 202. [PubMed]

61. Mason, J.O., III; Shah, A.A.; Vail, R.S.; Nixon, P.A.; Ready, E.L.; Kimble, J.A. Branch retinal artery occlusion: visual prognosis. *Am. J. Ophthalmol.* **2008**, *146*, 455–457. [CrossRef] [PubMed]

62. Hollenhorst, R.W. Significance of bright plaques in the retinal arterioles. *JAMA* **1961**, *178*, 23–29. [CrossRef] [PubMed]

63. Cackett, P.; Htoon, H.; Wong, D.; Yeo, I. Haemorrhagic pigment epithelial detachment as a predictive feature of polypoidal choroidal vasculopathy in a Chinese population. *Eye* **2010**, *24*, 789–792. [CrossRef] [PubMed]

64. Sowka, J.W.; Kabat, A.G. Collateral damage: In addition to vein occlusion, collateral vascularization may be linked to optic disc drusen, diabetes or even tumor formation. By Joseph W. Sowka, OD, and Alan G. Kabat, OD. *Rev. Optom.* **2014**, *151*, 85–88.